EASR

Engineering and Applied Science Research

https://www.tci-thaijo.org/index.php/easr/index

Published by the Faculty of Engineering, Khon Kaen University, Thailand

Safety of a bridge span with prestressed concrete beams

Assylkhan Jalairov[1)], Dauren Kumar[2)], Gulzhan Nuruldaeva*[3)], Sarsembekova Zeynep[2)], Shalkarov Abdiashim[1)] and Samal Karasai[4)]

[1)]The Kazakhstan Road Research Institute, Almaty, 050013, Republic of Kazakhstan
[2)]Al-Farabi Kazakh National University, Almaty, 050013, Republic of Kazakhstan
[3)]Satbayev University, Almaty, 050013, Republic of Kazakhstan
[4)]International University of Transportation and Humanities, Almaty, 050013, Republic of Kazakhstan

Received 3 January 2025
Revised 27 May 2025
Accepted 11 June 2025

Abstract

This article assesses the structural performance of a bridge overpass with a new type of reinforced concrete prestressed T-beams (TBN - abbreviation for stressed T-beams). Compared with VTK bridge beams (VTK - abbreviation: high-tech transportation construction), prestressed T-beams have technological advantages in the production process and during installation that allow for increased spacing, from 1400 mm for high-tech transport structure type beams to 2200 mm for prestressed T-beams. The study aims to evaluate the reliability of 24-m long prestressed T-beams and operation of their joints as part of a bridge overpass. Static testing of a bridge overpass was carried out using vehicles, with measurement of true deflections of the experimental beams and investigation of the operation of their joints as a part of the overpass. The calculated deflection values are determined using the finite element method in the Midas Civil software package. Test results showed the true and calculated deflections. The structural coefficients for the first and second test schemes were 0.79 and 0.81, respectively. This meets structural requirements. The structural coefficient is a criterion corresponding to the required load capacity for reliable operation of a structure under various force combinations.

Keywords: Overpass, 24-m prestressed T-beams, Finite element method, Midas Civil software, Tests

1. Introduction

A bridge overpass in the current study consists of 24-m long prestressed reinforced concrete T-beams. There are seven beams in the overpass cross-section. They are installed with 2.0 m (edge beam) and 2.2 m (middle beam) spacing. Prestressed T-beams [1-3] have several advantages over high-tech transport structure type beams that aid optimization of labor-intensive processes, both in manufacturing the beams and constructing overpasses. Heavy-weight concrete, according to GOST 26633–2015 [4], has a compressive strength of at least the B40 class. It is used for the manufacture of these beams. Modern plasticizers are employed in the manufacture of 24 -m prestressed T-beams. This is to ensure the required workability and water permeability. Seven-wire 15.2 mm diameter high tensile steel adhering to the ST RK EN 10138-3-2011 [5] standard was used as prestressed rebar. More information on the characteristics of prestressed T-beams and beams of this high-tech transport structure type can be found on the manufacturer's website [6] and elsewhere. VTC-24 m beam test results are presented in this article [7].

Earlier studies [8-10] numerically and experimentally considered the effectiveness of new beam structures. The effectiveness of concrete modifications with organic and mineral admixtures was investigated [11].

The overpass above bridge piers No. 2 and No. 3 is combined into temperature-continuous slabs to reduce the number of expansion dams. This allows for the smooth passage of vehicles along the structure's roadway. The temperature-continuous slabs are made by combining roadway slabs of the overpass beams in pier sections. They operate as continuous structures under horizontal and temperature effects, and as split structures under vertical effects.

The total length of the three-span bridge is 72.2 meters. It is in the Zhambyl region of Kazakhstan on the Khantau-Burylbaytal Road. The roadway is 11.5 m wide (two lanes, 3.75 m each, with two emergency lanes, which are each 2.0 m wide). The service walkways are each 0.75 m wide. The bridge is located on a straight section of the road. It crosses a railway at a 90° angle. A view of the road bridge over a railway is shown in Figure 1.

The bridge abutments are buried, reinforced in concrete, and abutment caps unite the upper ends of the columns. Circular 1.5 m diameter cross-section columns are used. There are four columns in each abutment. The distance between the columns is 3.8 m. The backwall of the abutment has 3.0 m long wing walls.

*Corresponding author.
Email address: g.nuruldaeva@satbayev.university
doi: 10.14456/easr.2025.41

Figure 1 The bridge in the current study.

2. Assessment of the technical condition of the bridge

The study of the serviceability of the TBN beams was aimed at determining beam behaviour as part of the span structure. Their safe operation was assessed along with compliance the design and regulatory requirements. Twenty-four-meter prestressed T-beam serviceability and the bridge itself were assessed following SP RK 3.03-113-2014 [12], the code of practice requirements.

Figure 2 shows a view of the 24-m prestressed T-beams and pier No. 3. Seven 24-meter prestressed T-beams were installed in three bridge spans following the project design.

Figure 2 View of pier No. 3 and the embankment cone of abutment No. 4.

Inspection of the 24-m prestressed T-beams showed that they have no defects. Measurements of the geometric dimensions of piers No. 2 and No. 3 showed that they adhered to the working design. The concrete surfaces of piers No. 2 and No. 3 are satisfactory and meet the project requirements. Anti-seismic devices are installed on the caps of piers No. 2 and No. 3 to prevent the displacement and falling of the 24-m prestressed T-beams in the event of an 8.0 intensity earthquake.

Aerodynamic stability issues of the bridge when subjected to high wind speeds are presented in [13, 14]. The advantages of using composite materials in bridge load-bearing structures are presented in [15]. Types of suitable bridge support structures for composite materials are given in [15].

The results of geodetic measurements showed that transverse and longitudinal slopes of the roadway ensure rainwater removal. Instrumental measurements were employed to observe vertical and horizontal displacements of the overpass, bridge piers, and abutments. These measurements allow the timely discovery of defects that cannot be detected during inspection, explain the occurrence of defects found during inspection, and the choice of the most appropriate ways to repair and strengthen structures [16-18].

3. Overpass testing

3.1 Test load calculation

The bridge overpass consists of seven 24-m prestressed T-beams. These T-beams are joined together in the transverse direction with the support of monolithic reinforced concrete slabs using connection bars from the roadway slabs of the T-beams. The structural behavior of the bridge overpass is analyzed under two loading cases.

In the first case, the basic load from vehicles is assessed from two lanes of an A14 load shifted to the emergency lane. The longitudinal axis of the outer lane A14 load is assumed to be 1.5 m from the emergency lane edge. The distance between the axes of the load lanes is 3 m. A14 load trailers are placed in the middle of the bridge overpass (see Figure 3). An A14 vehicular load is modeled in distributed traffic lanes, each of which includes one two-axle bogie with an axle load of 140 kN and evenly distributed load intensity on both tracks of -14 kN/m.

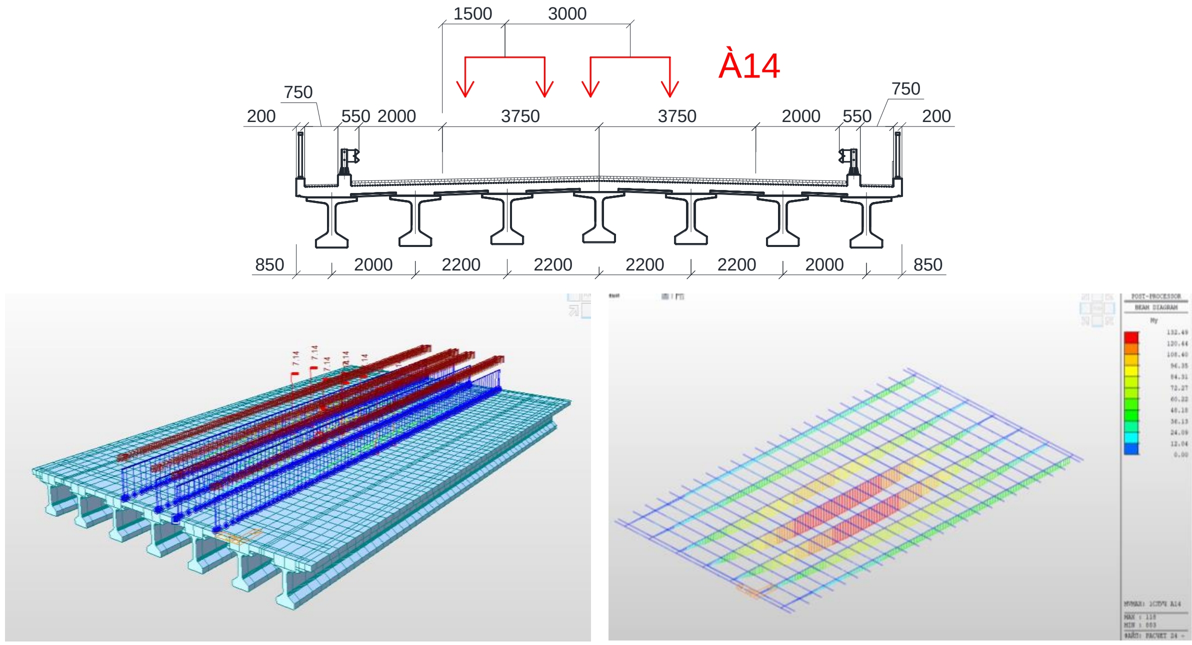

Figure 3 Diagram of M_y bending moments during overpass loading with an A14 load (the first load case).

In the second case, the load from vehicles is taken in the form of two lanes of A14 loads, shifted to the roadway edge, including the emergency lane. The longitudinal axis of the outer lane of the A14 load is assumed to be 1.5 m from the road barriers. The distance between the truck lane axes is assumed to be 3 m. A14 load trailers are placed in the middle of the bridge overpass (see Figure 4).

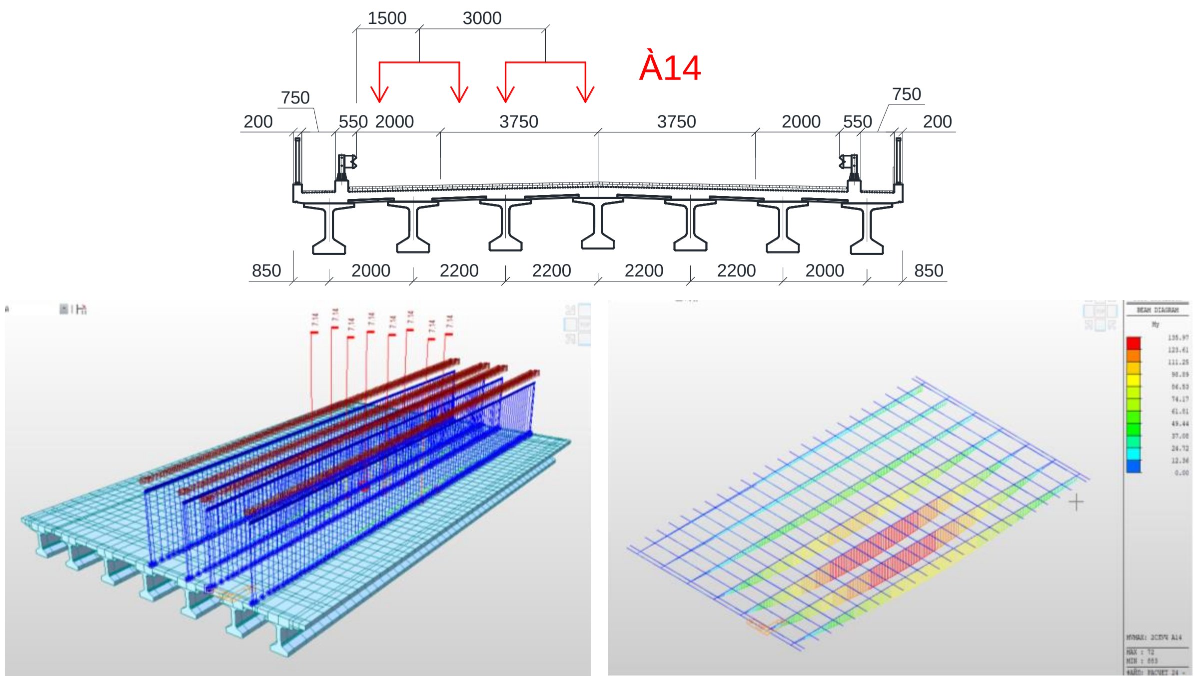

Figure 4 Diagram of M_y bending moments during overpass loading with an A14 load (the second load case).

Figures 3 and 4 show the location of temporary A14 loads across the bridge axis and the results of computer calculations performed in Midas Civil software. Table 1 shows the initial data for the calculation and values of certain maximum bending moments at the mid-span of a beam with a load reliability factor of one (y_f =1.0) and a total dynamic coefficient ((1+ μ)>1.0).

Table 1 Initial data and values of calculated bending moments for the first and the second cases of temporary A14 loading

Basic load		**Load reliability factor**		**Dynamic coefficient**	**Maximum bending moments at the mid-span of beam, kNm**	
For trailer kN	**For uniform load kNm**	**For trailer**	**For uniform load**		**The first load case**	**The second load case**
					when γ_f=1; 1+μ>1	
140	14	1.0	1.0	1.16	$M^1_{cal.max}$ =1325	$M^2_{cal.max}$ =1360

The overpass spatial design model in Midas Civil software was presented as a girder grillage and composed of general-type beam elements with the geometric and stiffness characteristics of an L-shaped cross-section corresponding to real prestressed reinforced concrete beams. In the transverse direction, the load-bearing beams were combined at the slab level with beam elements that simulate the work of combining structures along a monolithic reinforced concrete slab located at the roadway level.

In the next stage, boundary conditions were set in the spatial model, i.e., support conditions of the overpass beams. Since effective polyurethane-free bearings were adopted as supports to provide rotation of the beam sections and their mobility under force, it is possible to influence beam torsion in their support zone.

Following paragraph 7.2.7 of SP RK 3.03-113-2014, the forces arising in the load-bearing structures of road bridges from test load action should range from 70–100% of the calculated forces from mobile temporary vertical load action adopted in the project. Overpass loading was done with two test loads, as described below.

In the first scheme, the overpass is loaded with four vehicles. The longitudinal axis of the outermost vehicle is located 1.5 m from the roadway emergency lane. The distance between the axles of the vehicles in the transverse direction is 3.0 m. Thus, the first case of bridge structure loading with an A14 load is simulated (see Figure 5).

In the second scheme, the overpass is loaded with four vehicles. The longitudinal axis of the outermost vehicle is located 1.5 m from the roadway barrier. The distance between the vehicle axles in the transverse direction is 3.0 m. Thus, the second case of bridge structure loading with an A14 load is simulated (see Figure 6).

Figures 5 and 6 show the design schemes for loading a 24-m long overpass with test loads and computer calculation results.

For the first loading scheme:

$$\frac{M^1{}_{e.max}}{M^1_{cal.max}} = \frac{1172}{1325} = 0{,}884\ (88{,}4\ \%)$$

For the second loading scheme:

$$\frac{M^2{}_{e.max}}{M^2_{cal.max}} = \frac{1204}{1360} = 0{,}885\ (88{,}5\ \%)$$

Table 2 summarizes the calculation results under the test loads.

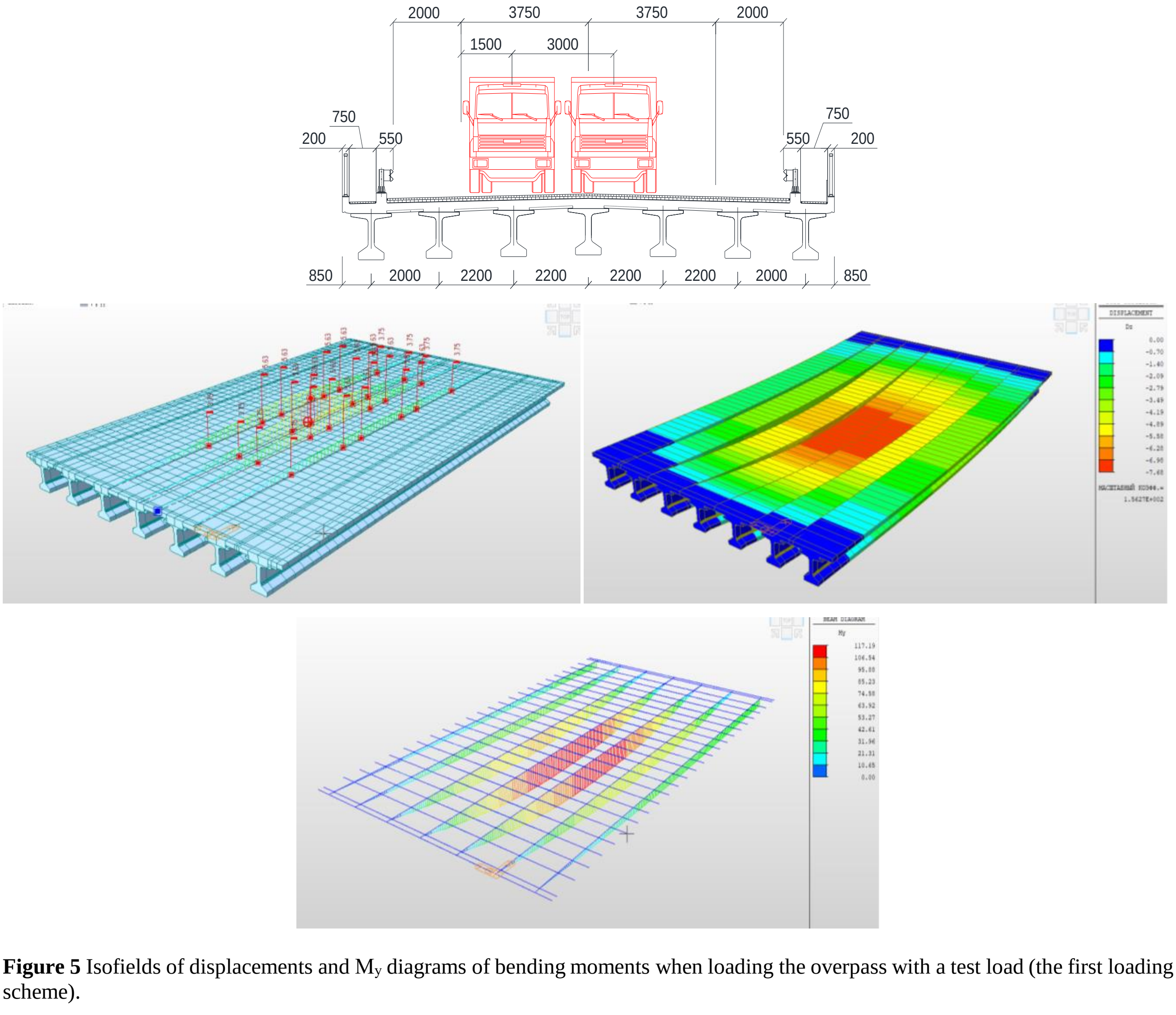

Figure 5 Isofields of displacements and M_y diagrams of bending moments when loading the overpass with a test load (the first loading scheme).

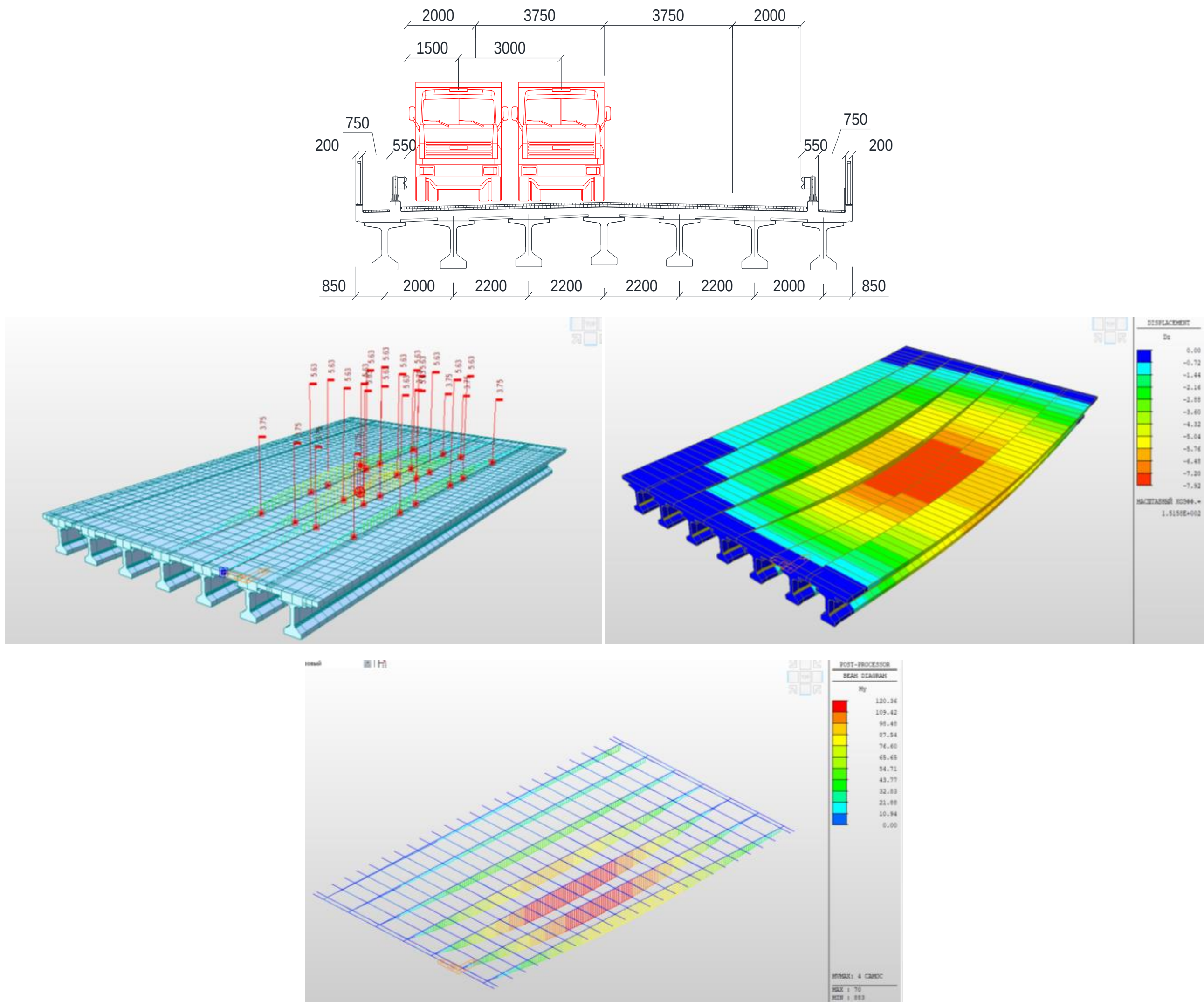

Figure 6 Isofields of displacements and M_y diagrams of bending moments when loading the overpass with a test load (the second loading scheme).

Table 2 Bending moments at the mid-span of a prestressed T-beam from test loading

TEST LOAD	
Maximum test bending moment at the mid-span of the beam	
The first loading scheme	**The second loading scheme**
$M^1_{e.max}$ =1172 kN·m	$M^2_{e.max}$ =1204 kN·m

The permissible maximum bending moments from temporary A14 loading with a reliability factor equal to one (γ_f =1.0) and a total dynamic coefficient ((1+ μ)>1.0) are - $M^1_{calc.max}$ =1325 kNm (the first loading scheme) and – $M^2_{calc.max}$ =1360 kNm (the second loading scheme) (see Table 1). The maximum bending moments from test load action are - $M^1_{e.max}$ = 1172 kNm (the first loading scheme) and $M^2_{e.max}$ = 1204 kNm (the second loading scheme) (see Table 2).

Thus, the adopted values of test loads comply with paragraph 7.2.7 of SP RK 3.03-113-2014 requirements. The test load is four vehicles with an average weight of 300 kN. The results of this calculation are considered.

Numerical modeling results of reinforced concrete beams using solid finite elements for modeling concrete and rod elements, accounting for crack propagation, are presented in [19]. Calculation of bridge overpass factors using software packages is presented in [1, 20]. The main parameter determining the possibility of operation is the load-bearing capacity of the bridge structure [21].

3.2 Bridge testing

During static tests of the bridge, Shacman and Howo trucks with ballast were used as test loads. Their weight was 300 kN each. Static tests of the 24-m-long overpass No. 1 were carried out following the work program. Two testing schemes were adopted. Four loaded vehicles with 300 kN ballast were slowly placed on the roadway, with the axis of the outermost vehicle located 1.5 m away from the emergency lane (see Figure 7), following the first test scheme.

Figure 7 View of the bridge roadway with test loads in the form of loaded vehicles (the first loading scheme).

According to the second test scheme, four loaded vehicles with 300 kN ballast were also placed in stages on the bridge roadway. However, in this case, the longitudinal axis of the outermost vehicle was 1.5 m from the roadway barriers (see Figure 8). Benkelman beams were used during testing to determine deflections in the seven overpass No. 1 beams (see Figure 9).

Figure 8 View of the bridge roadway with test loads in the form of loaded vehicles (the second loading scheme).

Figure 9 View of installed Benkelman beams.

Overpass No. 1 was loaded in stages, and beam deflections were recorded at each stage of loading. Figures 10 and 11 depict overpass No. 1 with loaded vehicles during static tests. These figures show the test deflections at the mid-span of 24-m-long prestressed T-beams recorded during static tests.

The test results in Figures 10 and 11 show the following:

- Deflections of the beams during loading and unloading had smooth outlines, which indicated the elastic behavior and the joints of the beams working as part of the overpass.

- The maximum deflections in one of the tested beams were 6.1 and 6.4 mm in the first and second test schemes, respectively.

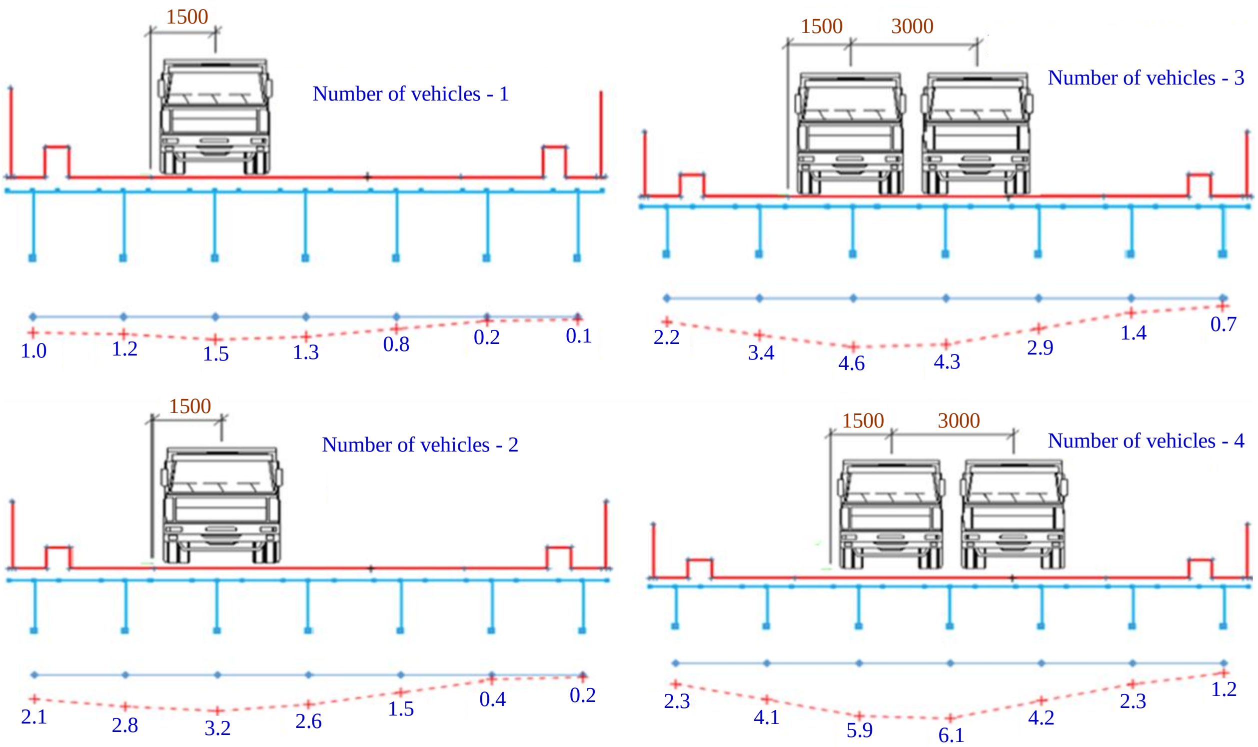

Figure 10 Experimental deflections at the mid-span of the beam under the first loading scheme (values in mm).

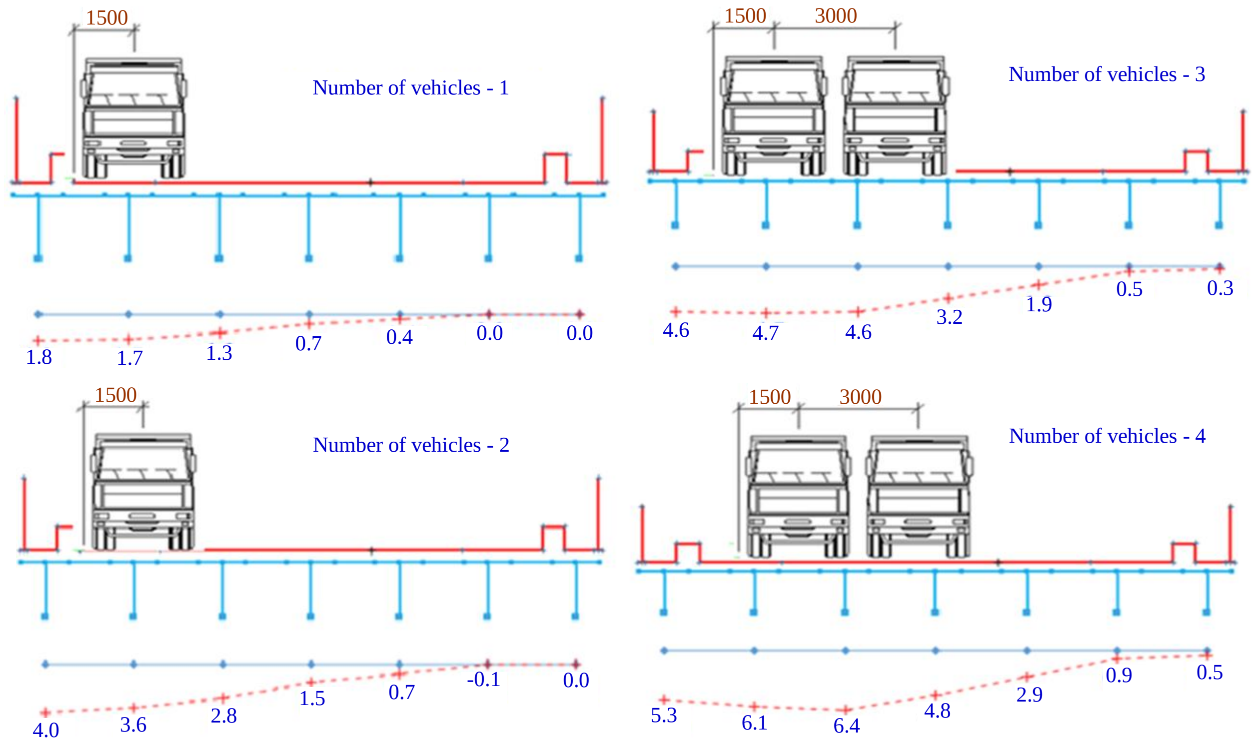

Figure 11 Experimental deflections at the mid-span of the beam under the second loading scheme (values in mm).

The main criterion for the operation of overpasses when testing a bridge structure is the agreement of elastic deflection measurements and calculated deflections of beams under the same test load. An indicator of the overpass beam operation during acceptance tests is the structural coefficient, following paragraph G.5.2 of Appendix G of SP RK 3.03-113-2014 Code of Practice, defined by the formula:

$$К = \frac{f_e}{f_{cal}}$$

f_e – experimental deflection of the beam from the test load
f_{cal} – calculated deflection of the beam from the test load

According to the test results, k structural coefficient values for the main load–bearing structures and their elements should be within 0.7–1.0.

3.3 Bridge testing results

Table 3 shows the bridge testing results.

Table 3 Experimental and calculated deflections with structural coefficients

Bridge	**Experimental maximum deflection value, f_e, mm**	**Calculated maximum deflection value, f_{cal}, mm**	**Structural coefficient, K**
First testing scheme	6.1 (see Figure 10)	7.7 (see Figure 9)	0.79
Second testing scheme	6.4 (see Figure 11)	7.9 (see Figure 10)	0.81

The K structural coefficients for the main load-bearing structures should be from 0.7–1.0 according to paragraph G.5.2 of Appendix G of SP RK 3.03-113-2014 Code of Practice “Bridges and Culverts. Rules of Examination and Testing”. The values of the structural coefficients obtained in the tests indicate that the structure functions according to the calculation models required by the project and regulatory documents.

The bearing and structural elements of the bridge were examined before the static tests, as well as after their completion. Inspections showed the absence of damage to the load-bearing structures caused by the test loads.

4 Conclusions

Several conclusions can be drawn from the results of this study. They include:

- Analysis of the technical condition assessment of the bridge structure showed no significant shortcomings or construction defects that could affect the design capacity of the bridge.
- Static load testing of Overpass No. 1 with 24-m prestressed T-beams confirmed the adequacy of the adopted test methodology. The key evaluation parameter, the structural coefficient defined in paragraph G.5.2 of Appendix G of SP RK 3.03-113-2014, was used to verify beam serviceability.
- The K structural coefficient value for the bridge main load-bearing structures should be 0.7–1.0 according to paragraph G.5.4 of the SP RK 3.03-113-2014 Code of Practice. Structural coefficient values of 0.79–0.81 were obtained in the bridge overpass static tests.
- The obtained values of the structural coefficients indicate that the overpass operates according to the project and regulatory requirements.
- Comparison of the measured and calculated deflections showed good agreement, indicating that the actual structural response under loading matches the design assumptions.
- The design bearing capacity of the road bridge is achieved, and the bridge can be operated under A14, NK-120, and NK-180 loads with no restrictions.

5. References

[1] Jalairov A, Kumar D, Kassymkanova KK, Murzalina G, Jangulova G. Ensuring operational reliability of overpass on "Almaty-Kapshagai" highway section in Kazakhstan. Commun - Sci Lett Univ Zilina. 2022;24(1):D23-36.

[2] Jalairov A, Kumar D, Nuruldaeva G, Kassymkanova KK, Kumar B, Zhalgasbekov Y. Inspection and preparation for testing of the road overpass of the Almaty-Kapshagai highway after the vehicular impacts. Commun - Sci Lett Univ Zilina. 2022;24(4):D160-73.

[3] Jalairov A, Kumar D, Kassymkanova KK, Nuruldaeva G, Imankulova A. Structural behavior of prestressed concrete bridge girder with monolithic joint. Commun - Sci Lett Univ Zilina. 2022;24(4):D150-9.

[4] Interstate Standard GOST 26633-2015. Heavy-weight and sand concretes. Specifications. Moscow: Standartinform Publ; 2019. (In Russian)

[5] Ministry of Investments and Development of the Republic of Kazakhstan. ST RK EN 10138-3-2011. Prestressing steels. Part 3. Strand. Almaty: Ministry of Investments and Development of the Republic of Kazakhstan; 2014. (In Russian)

[6] azmk.kz [Internet]. Almaty: Almaty plant bridge structures; 2015 [cited 2015 Dec 11]. Available from: http://www.azmk.kz/files/catalog_azmk_2017.pdf. (In Russian)

[7] Kumar DB, Kadyrmanov KA, Takenova DA. Influence of concrete age on buckling of bridge reinforced concrete girder VTK-24U. Industrial transportation in Kazakhstan. 2018;4(61):73-80. (In Russian)

[8] Moravcik M, Bujnakova P. New precast bridge girder with combined prestressing. Commun - Sci Lett Univ Zilina. 2011;13(3):19-23.

[9] Moravcik M. The load testing and numerical verifying of the precast prestressed girder. Commun - Sci Lett Univ Zilina. 2007;9(3):56-62.

[10] Jalairov A, Kumar D, Dosaev N, Nuruldaeva G, Kassymkanova KK, Murzalina G. Calculation and testing of a reinforced conical bridge beam. Archit Eng. 2023;8(2):33-48.

[11] Pshinko O, Shcherbak A, Rudenko D. Research of operational properties of modified specialized concrete for transport constructions. Commun - Sci Lett Univ Zilina. 2019;21(4):90-6.

[12] Ministry of national economy of the republic of Kazakhstan. SP RK 3.03-113-2014: Bridges and culverts. Rules of examination and test. Almaty: Ministry of national economy of the republic of Kazakhstan; 2014. (In Russian)

[13] Poddaeva O, Churin P, Loktev A, Salame CT. Stability and reliability of long-span bridge structure. Archit Eng. 2022;7(3):65-75.

[14] Poddaeva O, Churin P. Aerodynamic stability of bridges with various levels of structural damping. Archit Eng. 2021;6(4):54-62.

[15] Shendrik V, Kvitko A. Analysis of applicability of composite materials in supporting constructions of bridges. Archit Eng. 2016;1(3):29-32.
[16] Rabi M, Cashella KA, Shamass R. Flexural analysis and design of stainless steel reinforced concrete beams. Eng Struct. 2019;198:109432.
[17] Yu Y, Lee S, Cho JY. Deflection of reinforced concrete beam under low-velocity impact loads. Int J Impact Eng. 2021;154:103878.
[18] Kovacic B, Kamnik R, Pustovgar A, Vatin N. Analysis of precision of geodetic instruments for investigating vertical displacement of structures. Procedia Eng. 2016;165:906-17.
[19] Nazarenko SN, Grudcina GA. Method of the finite-element model formation containing the 3D elements for structural calculations of the reinforced concrete structures considering the crack opening. Commun - Sci Lett Univ Zilina. 2021;23(1):D15-25.
[20] Bujnakova P, Kralovanec J, Perkowski Z, Bouchair A. Verification of precast concrete girder bridge under static load. Civ Environ Eng. 2022;18(2):760-7.
[21] Vičan J, Odrobiňák J, Gocál J. Determination of road bridge load-carrying capacity. Civ Environ Eng. 2021;17(1):286-97.